Heliyon 10 (2024) e26776

Contents lists available at ScienceDirect

Heliyon

journal homepage: www.cell.com/heliyon

Research article

Use of buffer treatment to utilize local non-alkali tolerant bacteria in microbial induced calcium carbonate sedimentation in concrete crack repair

Satharat Pianfuengfoo [a], Sumonthip Kongtunjanphuk [b], Hexin Zhang [c], Piti Sukontasukkul [a,*]

[a] Construction and Building Material Research Center, Department of Civil Engineering, Faculty of Engineer, King Mongkut's University of Technology, North Bangkok, Thailand
[b] Department of Biotechnology, Faculty of Applied Sciences, King Mongkut's University of Technology, North Bangkok, Thailand
[c] School of Computing, Engineering and the Built Environment, Edinburgh Napier University, Edinburgh, Scotland, United Kingdom

ARTICLE INFO

Keywords:
Concrete
Crack repairing
Non-alkaline tolerant bacteria
Buffer treatment
Microbial induced calcium carbonate

ABSTRACT

Concrete often suffers cracks due to its low tensile strength. The repair process can vary ranging from surface coating, grouting, and strengthening. Microbial induced calcium carbonate sedimentation process (MICP) is a process of utilizing non-pathogenic bacteria to produce calcium carbonate through its urease activity in crack repair (filling). It is known as an alternative crack repair method that does not utilize Portland cement. In general, the bacteria used in MICP are alkali tolerant bacteria that have a higher chance of surviving the high alkalinity environment in concrete. However, in some regions, alkali tolerant bacteria are difficult to acquire and unavailable locally. This study introduced a technique to utilize non-alkali tolerant bacteria in MICP using buffer treatment. Instead of injecting bacteria directly onto the crack surface, the buffer solution was applied onto the crack surface prior to the bacteria injection. Results from the laboratory indicated a higher bacteria survival rate when the buffer treatment was applied to the medium. For the crack filling, with the buffer treatment, the crack was completely filled within 21–28 days. The microstructure results also showed that the crystal deposits from both laboratory and crack surface were similar in both physical appearance and phase composition.

1. Introduction

Concrete is the most used construction material worldwide due to its excellent compressive strength, raw material abundance, cost effectiveness, and high durability. However, concrete has a drawback concerning its brittle nature which makes it susceptible to cracking. Cracks in concrete come in various forms and sizes depending on the causes, such as improper loading conditions, poor design/construction practices, structural settlement, severe environmental conditions [1], etc. Attempts to prevent cracking in concrete include lowering water to cement (w/c) ratio, use of surface coating or hardening, use of steel reinforcement, and addition of random short fibers [2–7]. However, none of these methods can completely prevent cracking from occurring in concrete. Once concrete is cracked, without a proper repair treatment, it could lead to the seepage of moisture or harmful substances into the concrete,

* Corresponding author.
E-mail addresses: piti.s@eng.kmutnb.ac.th, piti@kmutnb.ac.th, piti.kmutnb@gmail.com (P. Sukontasukkul).

https://doi.org/10.1016/j.heliyon.2024.e26776
Received 28 June 2023; Received in revised form 19 February 2024; Accepted 20 February 2024
Available online 21 February 2024

Table 1
Classification of biological agents in risk groups.

Risk Group (RG)	Cause Human Disease	Treatment Available	Spread to Community
1	Unlikely	✓	Unlikely
2	Hazard	✓	Unlikely
3	Serious-hazard	✓	Risk of spreading
4	Serious-hazard	×	High risk of spreading

subsequently triggering the deterioration process of the structures [8–12].

Currently, there are various types of crack-repairing materials available commercially ranging from surface coating paint (enamel paints), polymer-based materials (epoxy resin), cement-based materials (grouting/non-shrink mortar, fast setting mortar), hybrid type (epoxy mortar), or concrete-based materials (fiber reinforced concrete, shotcrete, concrete overlay). The selection depends mainly on factors such as crack size, crack condition (active or non-active), strength requirement (filling or strengthening), compatibility with the existing concrete, etc. In terms of compatibility with the existing concrete, cement-based repairing materials are considered one of the most suitable choices due to the similarity in the modulus of elasticity and the coefficient of thermal expansion. However, the production of Portland cement is known to create several environmental issues such as greenhouse gases emissions, natural resource depletion, and fossil fuel consumption [13]. Therefore, the current trend on sustainable use of cement materials is moving toward lowering the Portland cement content or finding alternative cementitious material to entirely replace Portland cement. This also applies to the group of cement/mortar-based crack-repairing materials; a number of solutions have been proposed to reduce the cement content, for example, the use of pozzolan materials to partially replace cement content, the use of alternate cementitious material (polymer concrete, geopolymer) to completely replace cement content, and the use of microbial induced calcium carbonate sedimentation process (MICP) as a crack filler.

This study investigated the use of MICP as an alternate solution for crack filler by focusing on the use of local non-alkaline tolerant bacterium (NATB) available locally. Briefly, microbial induced calcium carbonate ($CaCO_3$) from MICP is a well-known metabolism process [14]. Ureolytic bacteria is are bacteria that produces urease enzymes to catalyze urea ($CO(NH_2)_2$) hydrolysis [15,16] to form carbamic acid (NH_2COOH), as shown in Eq. (1) [17].

$$CO(NH_2)_2 + H_2O \rightarrow NH_2COOH + NH_3 \quad (1)$$

Carbamic acid (NH_2COOH) spontaneously hydrolyzes with water to form carbonic acid (H_2CO_3) and ammonia (NH_3) (Eq. (2)) [18].

$$NH_2COOH + H_2O \rightarrow H_2CO_3 + NH_3 NH_2COOH + H_2O \rightarrow H_2CO_3 + NH_3 \quad (2)$$

The products are then equilibrated in water to form bicarbonate (HCO_3^-) and ammonium (NH_4^+) (Eqs. (3)–(5)) [19].

$$H_2CO_3 \leftrightarrow HCO_3^- + H^+ \quad (3)$$

$$2NH_3 + 2H_2O \leftrightarrow 2NH_4^+ + 2OH^- \quad (4)$$

$$HCO_3^- + H^+ + 2OH^- \leftrightarrow CO_3^{2-} + 2H_2O \quad (5)$$

The carbonate ions (CO_3^{2-}) finally react with the cell's surface calcium to form calcium carbonate ($CaCO_3$), which is also known as bio-cement (Eq. (6)) [20].

$$Cell\text{-}Ca^{2+} + CO_3^{2-} \rightarrow Cell\text{-}CaCO_3 \quad (6)$$

Although MICP is capable of self-producing calcium carbonate, the application in concrete crack-repairing is still far from practical use. There are a few limitations that need to be addressed, as follows:

- Biosafety concerns – some of the bacteria are known to be pathogenic, therefore, the restriction in biosafety is strongly enforced in MICP research and application.
- Growth rate in high pH environments – bacteria are generally neutrophiles. They grow best at neutral pH close to 7.0. The growth rate decreased when living in environments with pH > 7.0.

In terms of biosafety, Ivanov et al. [21] recommended the use of non-pathogenic bacteria only (Risk Group 1) and the risk group is classified based on Biological Agents Code of Practice 2020 [22], which divides bacteria into four risk groups – 1, 2, 3 and 4 (Table 1).

In the case of growth rate in high pH environments, most research related to MICP is often carried out using alkali-resistance bacteria. For example, Jongvivatsakul et al. [23] investigated crack healing using alkali-resistance *Bacillus sphaericus* LMG 2257. After 20 days of treatment, about 80% of the crack surface area was filled up. Chahal et al. [24] studied the influence of bacteria on the compressive strength of fly ash concrete. After 28 days, they found that alkali-resistance *Sporosarcina pasteurii* plays a significant role in increasing the compressive strength of fly ash concrete by up to 22%. Feng et al. [25] use alkali-resistance *Bacillus subtilis* M9 to heal 0.3 mm-width beam's bottom cracks. After curing for 28 days, the micro cracks were autonomously healed.

However, alkali-resistant bacteria are not readily available in most parts of the world. This is due to the lack of research activity

Table 2
Specification of bacteria.

Bacteria	Gram	Respiration	Maximum growth rate (hr.)	Risk group	Cause human disease
B. thuringiensis TISTR 126	positive	aerobic	32	1	Unlikely
B. megaterium TISTR 067	positive	aerobic	30	1	Unlikely
Bacillus sp. TISTR 658	positive	aerobic	17	2	Hazard
P. mirabilis TISTR 100	negative	anaerobic	12	2	Hazard
S. aureus TISTR 118	positive	aerobic	22	2	Hazard

related to them, making them barely available in the supply chain. Even though alkali-resistance bacteria can be isolated from alkali soils, the risk of contamination and the related cost is high. This leads to attempts to use non-alkali resistant bacteria in MICP research. For example, Khaliq et al. [26] experimented on a protective system by impregnating non-alkali resistant bacteria into porous aggregates before mixing with concrete. They found that the concrete incorporating bacteria directly did not show any effects in crack healing. The impregnation of bacteria in lightweight aggregates, on the other hand, showed consistency in their crack healing efficiency in specimens pre-cracked at later days. Erşan et al. [27] used a protective carrier to protect *Pseudomonas aeruginosa* and *Diaphorobacter nitroreducens* from the alkaline conditions to inhibit steel corrosion. Xu et al. [28] use ceramite to protect *Sporosarcina pasteurii* from the alkalinity. After 28 days, the 273-μm-width crack had a closure rate of 86%. Wang et al. [29] investigated the incorporation of highly urease-active strains of *Sporosarcina pasteurii* into recycled aggregates for the remediation of cracks in concrete. They found that incorporating bacteria into recycled aggregates could maintain the efficiency of the urea hydrolysis reaction and effectively heal the crack up to a width not exceeding 0.6 mm within 28 days. Han et al. [30] examined the embedding of *Bacillus cohnii* within ceramite. The results indicated the bacteria's ability to survive and successfully heal the crack, ranging from 0.47 to 0.48 mm within 56 days. Furthermore, Yuan et al. [31] studied incorporating zeolite with *Bacillus cereus* bacteria to heal the crack in concrete. The results showed that increased zeolite mass embedded with bacteria led to crack recovery by over 90% within 28 days.

Based on the literature review, although there are some studies related to MICP with non-alkali resistant bacteria, most of them focused on the use of protective systems to carry bacteria within concrete preventing them from coming into contact with the high pH environment [32]. This study, however, focuses on the use of buffer treatment to diminish the alkalinity (reduce the pH) of the repair area before starting the MICP process. The results showed that the buffer treatment improved bacteria survival and allowed the crack to fully heal within 21 days.

2. Experimental procedure

2.1. Bacteria strain and cultural process

In this research, five pure bacteria strains are acquired from Thailand Institute of Scientific and Technological Research (TISTR). The bacteria specification is given in Table 2. Nutrient Broth (NB) served as the base medium for the bacterial cultures utilized in this research, prepared at a concentration of 13 g/l, and sterilized in an autoclave at 121 °C for 15 min. This medium was employed to cultivate all bacterial strains this research investigated, including aerobic and anaerobic bacterial species. The cultivation of bacteria, concerning aerobic and anaerobic conditions, distinctly differs in this study. Bacterial cultivation by pipetting 1 ml of pure bacterial cultures in microcentrifuge tubes to a liquid medium of Nutrient Broth (NB) at a volume of 100 ml. Subsequently, this bacterial suspension was transferred to a multi-stacked refrigerated shaking incubator and incubated at 37 °C for the maximum growth rate. The difference in the cultivation of the respective bacterial types based on respiratory commenced from this stage. For the aerobic bacteria strains, shaking was employed during the cultivation period to facilitate oxygen replenishment for the aerobic bacteria at a rotational speed of 250 rpm. Conversely, the anaerobic bacteria strains did not require shaking to supplement oxygen during their cultivation.

To verify the respiration type of the bacterial strain, a preliminary experiment was conducted to observe bacterial growth under aerobic and anaerobic conditions. In this initial experiment, we attempted to incubate the selected anaerobic bacteria (*Proteus mirabilis* TISTR 100) under aerobic conditions (37 °C and shaking at 250 rpm). The results indicated that *Proteus mirabilis* cannot grow (did not turbid the Nutrient Broth) under aerobic conditions. However, growth was observed when it was incubated in an anaerobic environment; it thrived and settled at the bottom of the Erlenmeyer flask, exhibiting characteristics typical of anaerobic bacteria. In contrast, the remaining bacteria (aerobic type) on the list all exhibited growth in the presence of oxygen, causing the Nutrient Broth to become turbid.

According to the Biological Agents Code of Practice 2020, Table 1 classifies risk groups into four categories, with Group 1 considered non-pathogenic, and Groups 2 to 4 classified as hazardous and seriously hazardous. From the listed in Table 2, two bacterial strains, B. thuringiensis TISTR 12 and B. megaterium TISTR 067, fall under Risk Group 1 and are considered non-pathogenic. Details regarding risk groups and pathogenic characteristics are included in Table 2 for clarification.

2.2. Solution composition

In this research, five solutions were used that consisted of selective media nutrient broth (NB) mixing with urea, calcium chloride, phenol nitroprusside, alkaline hypochlorite, and pH9 buffer. Their compositions are shown in Table 3. The selective media consisted of a nutrient, as described in 2.1, used in the process of growing bacteria, and urea at a concentration of 20 g/l was utilized as an initial

Table 3
Selective media and solutions in this research.

Solutions	Compositions
Selective media [29,31,33]	Nutrient Broth (NB) 13 g/l Urea 2% w/v
Calcium chloride solution [33]	Calcium chloride dihydrate 0.10–0.30 M
Phenol nitroprusside solution [34]	Phenol 10 g/l Sodium nitroprusside 50 mg/l
Alkaline hypochlorite solution [34]	Sodium hydroxide 5 g/l Sodium hypochlorite (5% available chlorine)8.4 ml/l
pH9 buffer solution	Sodium tetraborate (borax) 0.025 M (100 ml) Hydrochloric acid 0.1 M (9.2 ml)

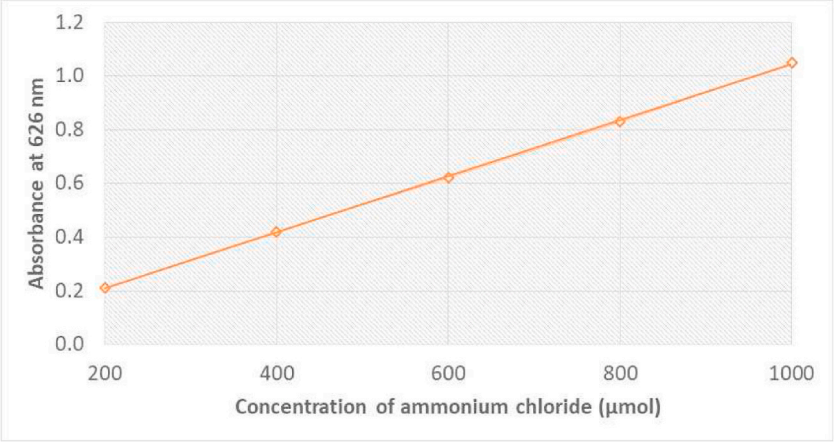

Fig. 1. Standard ammonium chloride curve.

substrate to produce urease enzyme. The calcium chloride solution was for initiating the MICP process. The phenol nitroprusside and alkaline hypochlorite solutions were used in measuring the urease activity. The last solution, the pH9 buffer, was an alkalinity-diminishing solution used in the crack healing process.

2.3. Measuring urease activity

The quantitative analysis of the urease enzyme was carried out based on Weatherburn's principle to estimate the amount of ammonia and urea from biological liquids [34]. First, the bacteria obtained from the culturing process were centrifuged at 4000 rpm at 4 °C for 30 min. Next, from the liquid floating on the top surface of the centrifuge, 0.25 ml was decanted into a vial using a micro-pipette. Then, 2.5 ml of 0.1 M urea and 1 ml of potassium phosphate buffer pH 8 were added to the vial by micropipette, and cured at 37 °C for 5 min. After that, 1 ml of alkaline hypochlorite and phenol nitroprusside solutions were added to the vial and incubated at 37 °C for 30 min. After the incubation, samples were subjected to an absorbance test (at 626 nm-wavelength) and the absorbance values were used calculate urease activity (in the form of unit enzyme U/ml).

The enzyme unit calculation involves a multi-step process, commencing with preparing an ammonium chloride standard solution curve, as shown in Fig. 1. This preliminary phase is crucial owing to urease's ability to hydrolyze urea into ammonia and ammonium, facilitating the detection of the initial urea's rate of change within 30 min from this standard solution curve. According to the principles of colorimetric change in the sample solution, after the preparation of the standard curve of the ammonium chloride solution, readings are obtained from the prepared samples using a spectrophotometer, measuring absorbance at a wavelength of 626 nm. When the absorbance readings exceed those within the standard solution curve, sample dilutions are performed, followed by recalibration of readings. After successful spectrophotometer readings, the absorbance values obtained are employed in the calculation to determine the concentration of the ammonium chloride solution (x) in Equation (7), which represents a linear equation (if the sample has been diluted, the dilution factor needs to be multiplied). The derived concentration value of the ammonium chloride solution (x) is then utilized in Equation (8) to compute the enzyme unit (U) per the volume of each specific initial substance and the duration of sample incubation to enable enzyme activity.

$$(y \times \text{dilution}) = ax + b \tag{7}$$

where, y is the reading $O.D._{626}$, x is an NH_4Cl (µmol)

Table 4
Cement mortar mix proportion.

Cement (kg/m^3)	Water (kg/m^3)	Fine aggregates (kg/m^3)
568	284	1420

$$\text{Urease activity} = \frac{x \times V_t}{V_{sub.} \times t_i \times V_{smp.}} \quad (8)$$

where, x is the NH_4Cl compute from the standard curve, V_t is the total volume (ml), $V_{sub.}$ is the volume of the substrate (ml), t_i is the incubation time (min.), $V_{smp.}$ is the volume of enzyme (ml).

2.4. Measuring microbial induced calcium carbonate crystal sedimentation

This process aimed to determine the optimal calcium chloride concentration suitable for each bacteria strain and its corresponding quantity of calcium carbonate sedimentation. Calcium chloride with five different concentrations were used: 100, 150, 200, 250 and 300 mM. For each concentration, the process began with aseptically adding 100 ml of calcium chloride to the bacterial-suspended solution (Section 2.1) followed by incubating each bacteria strain under respiratory conditions at 37 °C for 168 h. Finally, the solutions with calcium carbonate were vacuum filtered by Buchner funnel with Whatman's No.4 filter paper (15 μm), dried in a hot air oven at 60 °C for 24 h, and weighed.

Using the results from Sections 2.1 to 2.4, the non-pathogenic bacteria with the highest urease activity and high calcium carbonate crystal sedimentation were selected to use in the crack healing stage.

2.5. Bacteria survivability under alkaline cement environments with and without buffer treatment

The test in this part was divided into two parts:

1) Survivability under a high alkalinity environment without buffer treatment.

The objective of the first test was to determine the survivability rate of the bacteria under a high pH environment. The alkalinity of the cement's environment was simulated in the NB by adjusting the pH, ranging from 10 to 13 (gradually increased by 1) using 3 M sodium hydroxide (NaOH) solution. The cultivating process began by pipetting 1 ml of the selected bacteria strain liquid stock solution into the NB (100 ml) and incubating at 37 °C for maximum rate of growth. The growth rate is measured hourly based on the absorbance of bacteria at a wavelength of 600 nm from the exponential phase until it reaches the maximum and stationary phase, so the stationary point is used as the maximum growth rate. After reaching the maximum growth rate, the bacterial-suspended solution was taken out and subjected to an absorbance test at the wavelength of 600 nm. The cell concentration was calculated using Eq. (9) [33].

$$Y = 8.59 \times 10^7 \times Z^{1.3627} \quad (9)$$

where Z is the absorbance value reading at OD_{600}, and Y is the cell's concentration (cells/ml).

2) Survivability under a high alkalinity environment with buffer treatment

This part aimed to investigate the ability of a buffer to increase survivability of the selected bacteria strain under a high alkalinity environment. The buffer with a pH of 9 was prepared using 0.025 M sodium tetraborate (borax) (100 ml) and 0.1 M hydrochloric acid (9.2 ml). The testing process followed similar steps as described in Part 1, except that, before bacteria cultivation began, the high pH of the medium was adjusted by the buffer solution. At the end of cultivation, the samples were subjected to an absorbance test. The results in terms of cell concentration from 1) and 2) were compared and analyzed.

2.6. Crack treatment: sample preparation, treatment, and observation

Mortar samples in cubic form with dimensions of 100 × 100 × 100 mm were prepared using the mix proportion as shown in Table 4. To create an artificial crack, a 0.2 mm plastic sheet was inserted into fresh mortar at the top surface to the depth of 50 mm. After 120 min, the plastic sheet was removed, and the specimen was wrapped with plastic sheet until the test date.

The crack treatment began by injecting 1 ml of buffer solution onto the crack surface to reduce the surface alkalinity to about pH 9 followed by an injection of the bacterial-suspended solution of 1 ml into the crack. Then, the calcium chloride solution of 1 ml was injected into the crack at the same location. All the processes were aseptically controlled. The treatment process continued daily for 28 days. Crack observation was also performed daily at the same time and location.

Table 5
Urease activity.

Bacteria	Urease activity (U/ml)
B. thuringiensis TISTR 126	1722
B. megaterium TISTR 067	456
Bacillus sp. TISTR 658	522
P. mirabilis TISTR 100	2189
S. aureus TISTR 118	722

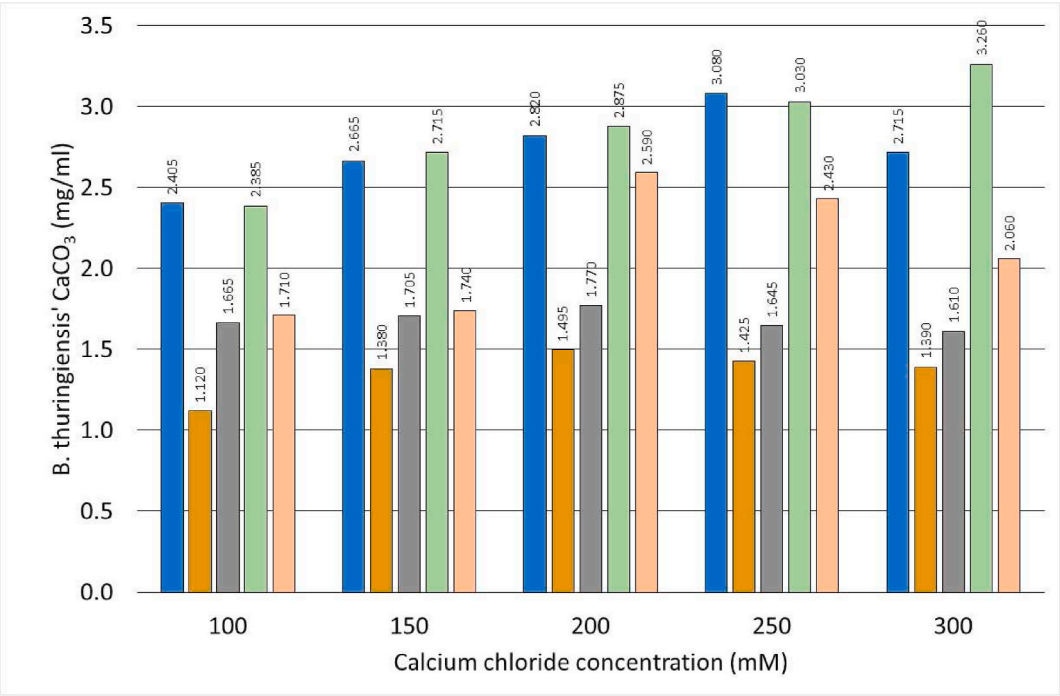

Fig. 2. Comparison of sedimented $CaCO_3$ of each bacteria strain.

2.7. Microstructural analysis

The microstructural and crystalline phase analysis was carried out using Scanning Electron Microscope (SEM) (FEI QUANTA 450) with a voltage of 10.0 kV 2000× magnification, X-Ray Diffractometer (XRD) (RIGAKU Smart Lab) with a scan range of 20–60° and Fourier Transform Infrared Spectroscopy (FITR) (PerkinElmer spectrum 2000) with a waveband range of 400–4000 cm^{-1}. The aim of this experiment is to compare the calcium deposits obtained from the laboratory (Section 2.4) and the crack surface (Section 2.6) with the pure $CaCO_3$. Therefore, the samples consisted of pure $CaCO_3$, and the sedimented crystal by the bacteria from the laboratory (Section 2.4), and from the crack surface (Section 2.6).

3. Results and discussion

3.1. Urease activity and $CaCO_3$ sedimentation

Table 5 shows the results on the urease activity of each bacteria strain, which was found to depend on the type of bacteria. From the results, the highest urease activity of 2189 U/ml was found in *P. mirabilis* TISTR 100, followed by *B. thuringiensis* TISTR 126, *S. aureus* TISTR 118, *Bacillus* sp. TISTR 658, and *B. megaterium* TISTR 067 at 1722, 722, 522, and 456 U/ml, respectively.

In the case of $CaCO_3$ sedimentation, the results are shown in Fig. 2. The sedimentation was found to depend on the type of bacteria and the calcium chloride ($CaCl_2$) concentration. In terms of $CaCl_2$ concentration, the quantity of $CaCO_3$ increased with the increasing $CaCl_2$ concentration up to a certain point then decreased. The concentration that yielded the highest $CaCO_3$ increment was designated as the optimum $CaCl_2$ concentration level and it was found to be different for each bacteria strain. For example, the *B. thuringiensis* TISTR 126 yielded the optimum $CaCl_2$ concentration at 250 mM, while the *B. megaterium* TISTR 067, *Bacillus* sp. TISTR 658, *and S. aureus* TISTR 118 yielded the same optimum concentration at 200 mM. For *P. mirabilis* TISTR 100, the highest yield was observed at $CaCl_2$ concentration of 300 mM.

Fig. 3. $CaCO_3$ sedimented by *B. thuringiensis* TISTR 126.

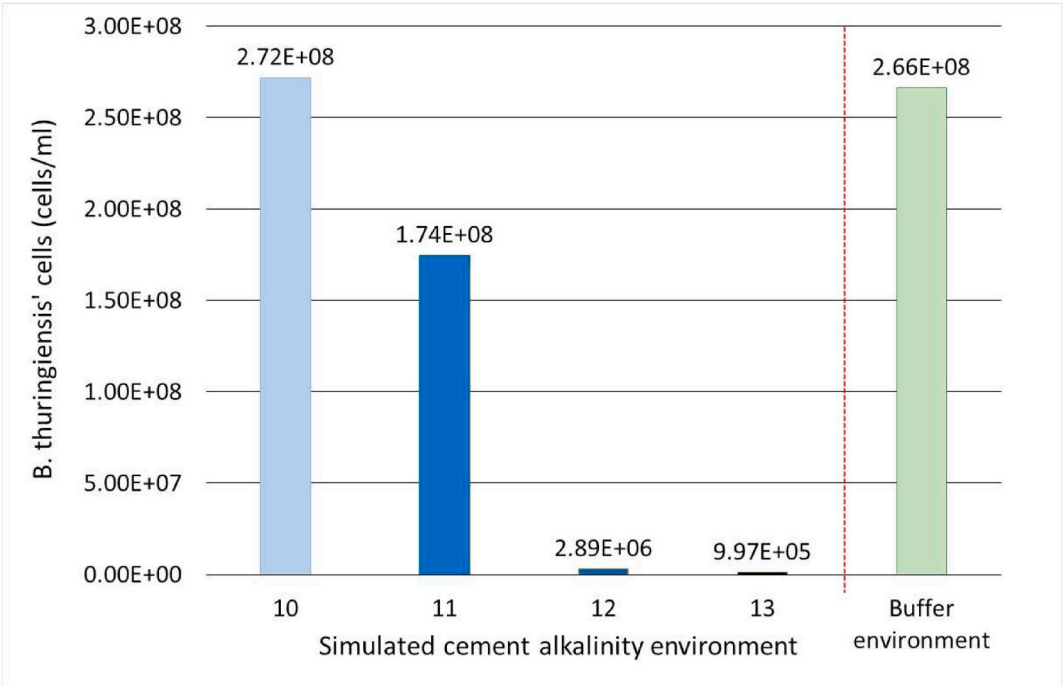

Fig. 4. Survivability of *B. thuringiensis* TISTR 126 under simulated cement alkalinity and buffer environments.

In terms of bacteria strain, the highest crystal yield was found in *P. mirabilis* TISTR 100 with 3.260 mg/ml at 300 mM $CaCl_2$ concentration, followed by *B. thuringiensis* TISTR 126 with 3.080 mg/ml at 250 mM. For *S. aureus* TISTR 118, *Bacillus* sp. TISTR 658, and *B. megaterium* TISTR 067, the highest increment was observed at 2.590, 1.770, and 1.495 mg/ml, respectively, at 200 mM. Based on the obtained results of both tests, the sedimented crystals appeared to follow the same trend to that of urease activity. This indicates that the bacteria that exhibited high urease activity also deposited large amounts of calcium carbonate.

Based on the selection criteria given in Section 2.3, the non-pathogenic *B. thuringiensis* TISTR 126 that yielded the highest $CaCO_3$ sedimentation and urease activity at 3.080 mg/ml and 1722 U/ml, was selected to continue to the next tests (survivability under high alkali environment and crack filling). The appearance of $CaCO_3$ sedimented from the selected bacteria strain was in flaky shape with a light-brown color, as shown in Fig. 3. It is noteworthy that the sedimented calcium carbonate resulting from the selected bacterial strain (B. thuringiensis TISTR 126) does not manifest as a white crystal, in contrast to observations in other studies. This indicates that different bacterial strains can produce calcium carbonate sediment with varying characteristics.

3.2. Survivability under cement alkalinity

Hardened cement, in general, has a pH value of about 11–13 due to the presence of calcium hydroxide from the hydration reaction.

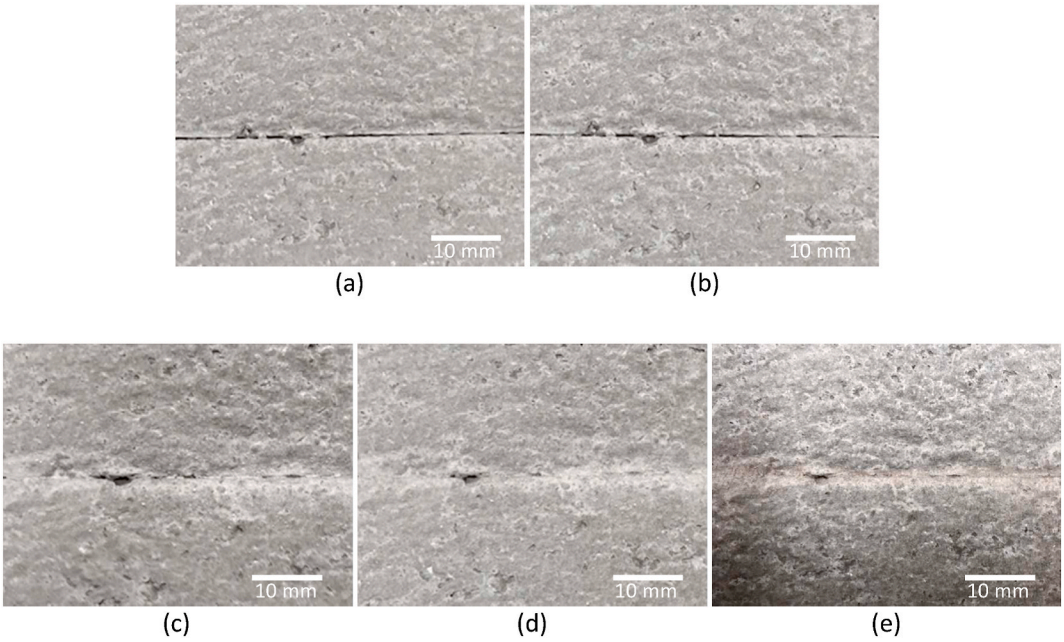

Fig. 5. Crack observation on the a) 1st, b) 7th, c) 14th, d) 21st, and e) 28th day of treatment.

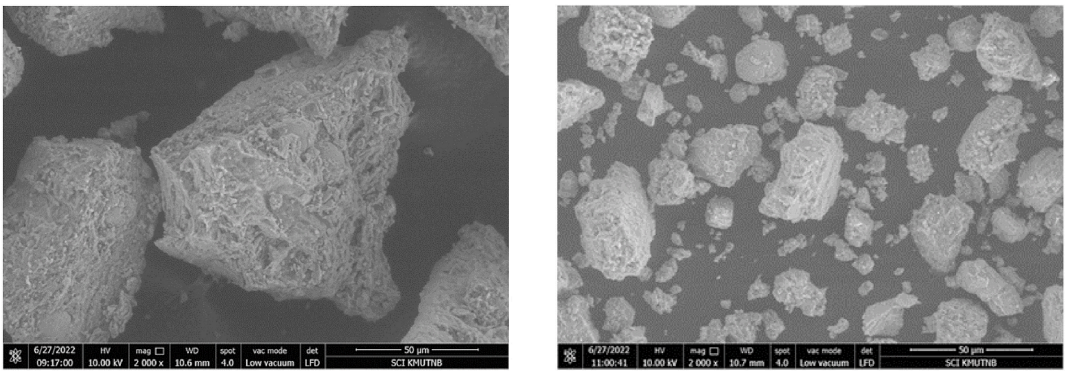

Fig. 6. The SEM microstructure images of the crystal deposits from the a) laboratory and b) crack.

However, most bacteria are known for stopping growth under high alkalinity environments. Therefore, it is necessary to test for survivability of the selected bacteria (*B. thuringiensis* TISTR 126). A high alkalinity environment with pH 10 to 13 was simulated in the laboratory. The bacteria were then cultivated using the process described in Section 2.5(1). The results are shown in Fig. 4. Based on the results, the number of bacteria cells decreased with the increasing pH value. At pH 10, the cell count was about 2.72×10^8 cell/ml and as the pH increased to 13, the cell count reduced significantly to about 9.97×10^5 cell/ml. This clearly indicates that the *B. thuringiensis* TISTR 126 cannot tolerate high alkalinity environments, especially at pH 13.

In the case of a buffer environment, the buffer treatment was used to adjust the pH of the simulated high alkali medium using the process described in Section 2.5(2). The results showed the cell count increased from 9.97×10^5 to about 2.66×10^8 cell/ml; almost equal to the cell count at pH 10. This implied that the buffer treatment allowed *B. thuringiensis* TISTR 126 to survive and grow under the high alkalinity environment.

3.3. Crack filling observation

Fig. 5 illustrates the change in physical appearance of the crack using the MICP process under the buffer treatment. At the early stage (1st and 7th day), almost no change occurred to the crack surface (Fig. 5a and b).The changes were observed after 14 days where solid particles began to gradually fill the surface crack (Fig. 5c). The crack was almost filled after 21 days of treatment (Fig. 5d), and completely filled after being treated for 28 days (Fig. 5e). The obtained results showed that the buffer treatment method allowed the non-alkali resistant bacteria (*B. thuringiensis* TISTR 126) to survive in the high alkalinity environment, which also allowed the MICP

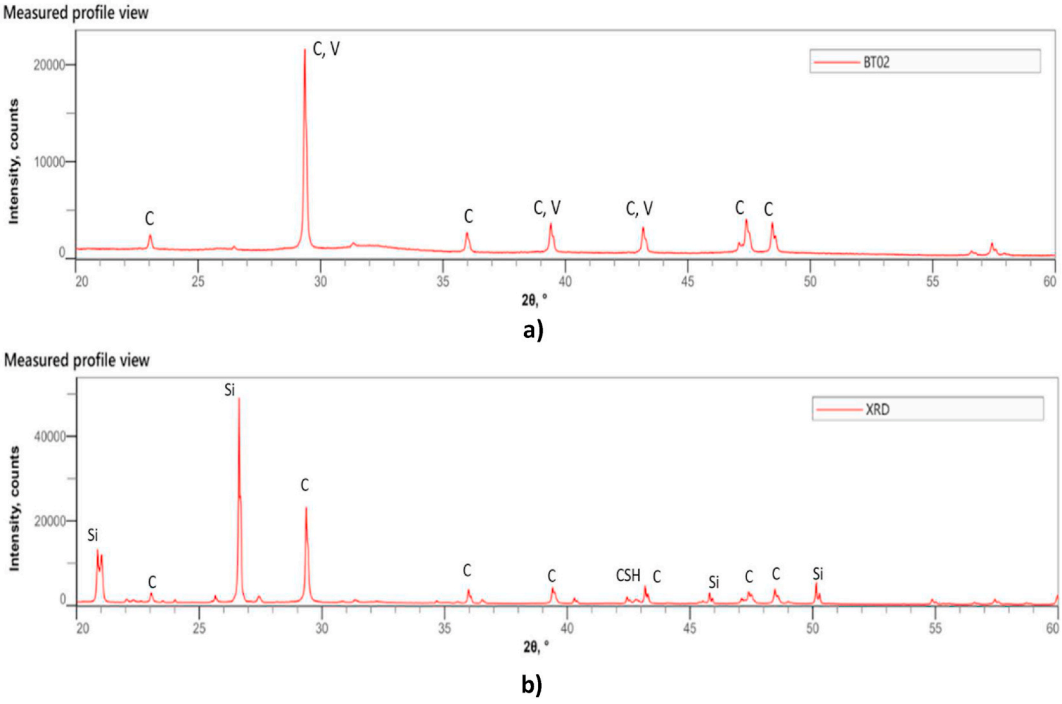

Fig. 7. Phase composition using XRD technique of the crystal deposit from the a) Laboratory and b) Crack surface.

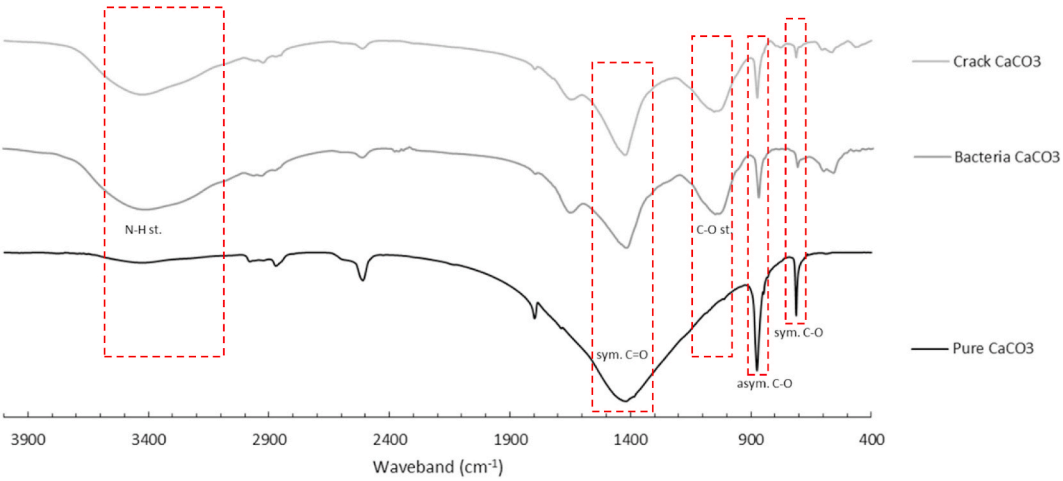

Fig. 8. Vibrational of each crystal using FTIR technique.

process to continue efficiently and to fill up the crack with calcium crystal sediment within 21–28 days.

Results from other researchers where alkali-resistant bateria were used with or without a protective carrier indicated that up to 80% of the crack can be filled within 20–28 days of treatment. For example, Jongvivatsakul et al. [23] used alkaline-resistant *Sporosarcina pasteurii* and observed that about 80% of the 0.4-mm-width crack could be filled up within 20 days. When using a protective carrier, Feng et al. [25] was able to entirely fill the 0.3-mm-width crack within 28 days using alkaline-resistant *Bacillus subtilis* M9. Xu et al. [28] showed that up to 86% of the 0.273-mm-width crack was filled within 28 days using *Sporosarcina pasteurii*.

Comparing between the proposed buffer treatment method using non alkali-resistant bacteria and the use of alkali-resistant bacteria, similar efficiencies can be obtained in terms of the duration of crack filling (20–28 days). However, the proposed method is more effective in terms of bateria strain availability.

3.4. Microstructure

The microstructure investigation included obtaining microstructure images using a SEM and phase composition using an XRD test. The objective is to compare both physical and phase composition of the microstructures between the crystal increment from the crack surface and the laboratory, to confirm that they are the same crystal sediment produced from the selected bacteria in the MICP process.

Results from the SEM test are shown in Fig. 6. The microstructure of $CaCO_3$ sediment is angular in shape with an average particle size of 79 μm, as shown in Fig. 6a. The physical appearance is a brown color with rough surface texture. Dhami et al. [35] also investigated the microstructure of the same bacteria in this study (*B. thuringiensis,* 25 mM $CaCl_2$) and the reported results were similar. In the case of crystal sediment from the crack surface, similar texture and shape were observed (Fig. 6b). However, the particle size obtained from the crack surface varied in size due to the process of acquiring the sample (scraping).

In terms of phase composition, the results are shown in Fig. 7. Fig. 7a shows the results from the laboratory samples; peaks were observed at 23.03°, 29.35°, 35.97°, 39.39°, 43.17°, 47.37°, and 48.44°, and the phase composited consisted mainly of calcite (C) and vaterite (V) [32]. For the samples from crack surface, the phase composition was found to consist of more minerals such as silicon dioxide (Si), calcite (C), vaterite (V), and calcium silicate hydrate (CSH) (Fig. 7b). However, considering the calcite phase, the peaks from the crack surface sample were observed at similar angles to those from the lab sample (listed above). This indicated that the crystal deposits from both sources are mainly calcium carbonate that produced the same bacteria (B. *thuringiensis* TISTR 126). As from the MICP. As for other minerals such as Si (26.62°) and CSH (42.5°), it is believed they come from the concrete base specimen, which were mixed together with the calcium sediment during the acquisition process.

In the context of confirming chemical structural groups using FTIR technique, as shown in Fig. 8, vibrational modes corresponding to carbonate ions were identified in all three samples at wavenumbers 712, 873, and 1420 cm^{-1}. These indicated symmetric C–O, asymmetric C–O, and symmetric C═O vibrations. However, noticeable differences arose from bacterial activity at the wavenumber 1052 cm^{-1} in the calcium carbonate sample, showcasing carbonate's distinctive C–O stretching structure. A prominent broad peak appeared in the 3500 to 3000 cm^{-1} waveband range, specifically in the calcium carbonate sediment from bacteria. This differentiation is likely derived from N–H stretching, potentially originating from amino acids within the bacterial structure, including compounds deriving from urea.

4. Conclusions

Based on the obtained results, the following conclusions can be drawn:

1) Among the five types of bacteria used in this study, the non-pathogenic *B. thuringiensis* TISTR 126 was found to produce the highest $CaCO_3$ sedimentation and urease activity at 3.080 mg/ml and 1722 U/ml. Each bacteria type responded differently to the different levels of calcium chloride concentration in terms of $CaCO_3$ sedimentation. The *B. thuringiensis* TISTR 126 responded well with a $CaCl_2$ concentration of 250 mM, while the *B. megaterium* TISTR 067, *Bacillus* sp. TISTR 658, and *S. aureus* TISTR 118 responded well with a $CaCl_2$ concentration of 200 mM.
2) The $CaCO_3$ sedimentation obtained from the MICP of *B. thuringiensis* TISTR 126 was a flaky-angular shaped powder with an average particle size of 79 μm and a light-brown color.
3) The growth rate of *B. thuringiensis* TISTR 126 decreased significantly under the high alkali environment with pH higher than 10. However, with buffer treatment, the survival rate increased to about the same as that under pH 10.
4) In terms of crack filling, based on visual inspection alone, with buffer treatment, the MICP using non-alkali-tolerant B. thuringiensis TISTR 126 appears capable of completely filling a 0.2-mm crack within 21–28 days. The calcium deposit from both sources (laboratory and crack surface) were confirmed to be the same in terms of physical appearance and phase composition. The phase composition was mainly calcite (C) with peaks at the same angles.

Data availability statement

Data will be made available on request.

CRediT authorship contribution statement

Satharat Pianfuengfoo: Writing – original draft, Investigation, Formal analysis, Data curation. **Sumonthip Kongtunjanphuk:** Writing – review & editing, Writing – original draft, Visualization, Validation, Supervision, Resources, Methodology, Conceptualization. **Hexin Zhang:** Writing – review & editing, Validation. **Piti Sukontasukkul:** Writing – review & editing, Writing – original draft, Validation, Supervision, Resources, Project administration, Funding acquisition, Conceptualization.

Declaration of competing interest

The authors declare the following financial interests/personal relationships which may be considered as potential competing interests:Piti Sukontasukkul reports financial support was provided by National Science, Research and Innovation Fund (NSRF). Piti Sukontasukkul reports financial support was provided by King Mongkut's University of Technology North Bangkok. Piti Sukontasukkul reports a relationship with National Science, Research and Innovation Fund (NSRF) that includes: funding grants. Piti Sukontasukkul

reports a relationship with King Mongkut's University of Technology North Bangkok that includes: funding grants. Piti Sukontasukkul, Satharat Pianfuengfoo, and Sumonthip Kongtunjanphuk has patent pending to Department of Intellectual Property, Thailand. No author has other relationship that may be interpreted as a conflict of interest by the reader. If there are other authors, they declare that they have no known competing financial interests or personal relationships that could have appeared to influence the work reported in this paper.

Acknowledgements

This research is funded by the National Science, Research and Innovation Fund (NSRF) and King Mongkut's University of Technology North Bangkok (KMUTNB) under the contract no. KMUTNB–FF–66-02. The author would like to thank Ruth Saint from Edinburgh Napier University for proofreading the manuscript.

References

[1] J. Xu, X. Wang, Self-healing of concrete cracks by use of bacteria-containing low alkali cementitious material, Construct. Build. Mater. 167 (2018) 1–14.
[2] P. Nuaklong, N. Boonchoo, P. Jongvivatsakul, T. Charinpanitkul, P. Sukontasukkul, Hybrid effect of carbon nanotubes and polypropylene fibers on mechanical properties and fire resistance of cement mortar, Construct. Build. Mater. 275 (2021) 122189.
[3] C. Chaikaew, P. Sukontasukkul, U. Chaisakulkiet, V. Sata, P. Chindaprasirt, Properties of concrete Pedestrian Blocks containing crumb rubber from recycle waste tyres reinforced with steel fibres, Case Stud. Constr. Mater. 11 (2019) e00304, https://doi.org/10.1016/j.cscm.2019.e00304.
[4] B. Maho, P. Sukontasukkul, S. Jamnam, E. Yamaguchi, K. Fujikake, N. Banthia, Effect of rubber insertion on impact behavior of multilayer steel fiber reinforced concrete bulletproof panel, Construct. Build. Mater. 216 (2019) 476–484, https://doi.org/10.1016/j.conbuildmat.2019.04.243.
[5] P. Sukontasukkul, S. Jamnam, M. Sappakittipakorn, N. Banthia, Preliminary study on bullet resistance of double-layer concrete panel made of rubberized and steel fiber reinforced concrete, Mater. Struct. 47 (1) (2014) 117–125.
[6] P. Sukontasukkul, S. Mindess, N. Banthia, Properties of confined fibre-reinforced concrete under uniaxial compressive impact, Journal of Cement and Concrete Research (JCCR) 35 (1) (2005) 11–18.
[7] P. Sukontasukkul, Tensile behaviour of hybrid fibre reinforced concrete, Adv. Cement Res. 16 (3) (2004) 115–122.
[8] Y. Li, X. Chen, L. Jin, R. Zhang, Experimental and numerical study on chloride transmission in cracked concrete, Construct. Build. Mater. 127 (2016) 425–435.
[9] Y. Zeng, Q. Zou, S. Jiang, M. Guo, T. Wang, H. Chu, Effect of CTAB on the healing of concrete cracks repaired by electrodeposition and the durability of repaired concrete, Construct. Build. Mater. 326 (2022) 126757.
[10] D. Liu, K. Cao, Y. Tang, A. Zhong, Y. Jian, C. Gong, X. Meng, Ultrasonic and X-CT measurement methods for concrete deterioration of segmental lining under wetting-drying cycles and sulfate attack, Measurement 204 (2022) 111983.
[11] Y. Huang, F. Ji, Z. Chen, J. Yu, Analytical solution for chloride diffusion in concrete with the consideration of nonlinear chloride binding, Construct. Build. Mater. 360 (2022) 129457.
[12] Y. Zheng, Y. Zhang, J. Zhuo, Y. Zhang, C. Wan, A review of the mechanical properties and durability of basalt fiber-reinforced concrete, Construct. Build. Mater. 359 (2022) 129360.
[13] R.M. Andrew, Global CO2 emissions from cement production, Earth Syst. Sci. Data 10 (2018) 195–217.
[14] Z. Wang, N. Zhang, G. Cai, Y. Jin, N. Ding, D. Shen, Review of ground improvement using microbial induced carbonate precipitation (MICP), Mar. Georesour. Geotechnol. 35 (8) (2017) 1135–1146.
[15] A. Talaiekhozani, A. Keyvanfar, R. Andalib, M. Samadi, A. Shafaghat, H. Kamyab, M.W. Hussin, Application of Proteus mirabilis and Proteus vulgaris mixture to design self-healing concrete, Desalination Water Treat. 52 (19–21) (2014) 3623–3630.
[16] P. Anbu, C.-H. Kang, Y.-J. Shin, J.-S. So, Formations of calcium carbonate minerals by bacteria and its multiple applications, SpringerPlus 5 (1) (2016) 250.
[17] R.A. Burne, Y.-Y.M. Chen, Bacterial ureases in infectious diseases, Microb. Infect. 2 (5) (2000) 533–542.
[18] F. Hammes, N. Boon, J. de Villiers, W. Verstraete, S.D. Siciliano, Strain-specific ureolytic microbial calcium carbonate precipitation, Appl. Environ. Microbiol. 69 (8) (2003) 4901–4909.
[19] Y. Fujita, J.L. Taylor, T.L.T. Gresham, M.E. Delwiche, F.S. Colwell, T.L. McLing, R.W. Smith, Stimulation of microbial urea hydrolysis in groundwater to enhance calcite precipitation, Environ. Sci. Technol. 42 (8) (2008) 3025–3032.
[20] C. Qian, R. Wang, L. Cheng, J. Wang, Theory of microbial carbonate precipitation and its application in restoration of cement-based materials defects, Chin. J. Chem. 28 (5) (2010) 847–857.
[21] V. Ivanov, V. Stabnikov, O. Stabnikova, S. Kawasaki, Environmental safety and biosafety in construction biotechnology, World J. Microbiol. Biotechnol. 35 (2019) 26.
[22] Health and Safety Authority, Biological Agents Code of Practice – Code of Practice for the Safety, Health and Welfare at Work (Biological Agents) Regulations 2013 and 2020, Dublin, Ireland, 2020. Nov. 2020).
[23] P. Jongvivatsakul, K. Janprasit, P. Nuaklong, W. Pungrasmi, S. Likitlersuang, Investigation of the crack healing performance in mortar using microbially induced calcium carbonate precipitation (MICP) method, Construct. Build. Mater. 212 (2019) 737–744.
[24] N. Chahal, R. Siddique, A. Rajor, Influence of bacteria on the compressive strength, water absorption and rapid chloride permeability of fly ash concrete, Construct. Build. Mater. 28 (1) (2012) 351–356.
[25] J. Feng, B. Chen, W. Sun, Y. Wang, Microbial induced calcium carbonate precipitation study using *Bacillus subtilis* with application to self-healing concrete preparation and characterization, Construct. Build. Mater. 280 (2021) 122460.
[26] W. Khaliq, M.B. Ehsan, Crack healing in concrete using various bio influenced self-healing techniques, Construct. Build. Mater. 102 (1) (2016) 349–357.
[27] Y.Ç. Erşan, H. Verbruggen, I.D. Graeve, W. Verstraete, N.D. Belie, N. Boon, Nitrate reducing CaCO3 precipitating bacteria survive in mortar and inhibit steel corrosion, Cement Concr. Res. 83 (2016) 19–30.
[28] J. Xu, X. Wang, J. Zuo, X. Liu, Self-healing of concrete cracks by ceramsite-loaded microorganisms, Adv. Mater. Sci. Eng. (2018) 5153041.
[29] X. Wang, J. Xu, Z. Wang, W. Yao, Use of recycled concrete aggregates as carriers for self-healing of concrete cracks by bacteria with high urease activity, Construct. Build. Mater. 337 (2022) 127581.
[30] R. Han, S. Xu, J. Zhang, Y. Liu, A. Zhou, Insights into the effects of microbial consortia-enhanced recycled concrete aggregates on crack self-healing in concrete, Construct. Build. Mater. 343 (2022) 128138.
[31] H. Yuan, Q. Zhang, X. Hu, M. Wu, Y. Zhao, Y. Feng, D. Shen, Application of zeolite as a bacterial carrier in the self-healing of cement mortar cracks, Construct. Build. Mater. 331 (2022) 127324.
[32] M. Luo, X. Li, Y. Liu, K. Jing, Application of artificial functional aggregates encapsulated bacteria for self-healing of cement mortars, J. Mater. Civ. Eng. 34 (11) (2022) 04022291.
[33] G.D.O. Okwadha, J. Li, Optimum conditions for microbial carbonate precipitation, Chemosphere 81 (9) (2010) 1143–1148.
[34] M.W. Weatherburn, Phenol-hypochlorite reaction for determination of ammonia, Anal. Chem. 39 (1967) 971–974.
[35] N.K. Dhami, M.S. Reddy, A. Mukherjee, Biomineralization of calcium carbonate polymorphs by the bacterial strains isolated from calcareous sites, J. Microbiol. Biotechnol. 23 (5) (2013) 707–714.